Science Translational Medicine
AAAS

www.sciencetranslationalmedicine.org/cgi/content/full/10/432/eaao1313/DC1

Supplementary Materials for

Brain-released alarmins and stress response synergize in accelerating atherosclerosis progression after stroke

Stefan Roth, Vikramjeet Singh, Steffen Tiedt, Lisa Schindler, Georg Huber, Arie Geerlof, Daniel J. Antoine, Antoine Anfray, Cyrille Orset, Maxime Gauberti, Antoine Fournier, Lesca M. Holdt, Helena Erlandsson Harris, Britta Engelhardt, Marco E. Bianchi, Denis Vivien, Christof Haffner, Jürgen Bernhagen, Martin Dichgans, Arthur Liesz*

*Corresponding author. Email: arthur.liesz@med.uni-muenchen.de

Published 14 March 2018, *Sci. Transl. Med.* **10**, eaao1313 (2018)
DOI: 10.1126/scitranslmed.aao1313

The PDF file includes:

Materials and Methods

Transient ischemia-reperfusion stroke model. Mice were anaesthetized with isoflurane delivered in a mixture of 30% O_2 and 70% N_2O. An incision was made between the ear and the eye in order to expose the temporal bone. A laser doppler probe was affixed to the skull above the middle cerebral artery (MCA) territory, and the mice were placed in supine position. A midline neck incision was made and the common carotid artery and left external carotid artery were isolated and ligated; a 2-mm silicon-coated filament (Doccol) was introduced via a small incision in the common carotid artery and inserted into the internal carotid artery, finally occluding the MCA which was confirmed by a corresponding decrease in blood flow (decrease in the laser doppler flow signal <20% of baseline value). After 60 minutes of occlusion, the animals were re-anesthetized, and the filament was removed. After recovery, the mice were kept in their home cage with facilitated access to water and food. Sham-operated mice received the same surgical procedure, except the filament was inserted and immediately removed, after 60 minutes mice were re-anesthetized. Body temperature was maintained at 37°C throughout surgery using a feedback-controlled heating pad. The overall mortality rate in this group (excluding the Sham-operated animals) was approximately 20 %. Exclusion criteria: 1. Insufficient MCA occlusion (a reduction in blood flow to >20% of the baseline value). 2. Death during the surgery. 3. Lack of brain ischemia as quantified post-mortem by histological analysis. A stroke assessment score was acquired 1 hour after reperfusion. For scoring the animal after surgical procedure a score from 0 (no stroke) to 5 (very severe stroke) based on general activity and body asymmetry was used ("modified Bederson Score") (*41*).

Splenectomy. Mice were anaesthetized with isoflurane delivered in a mixture of 30% O_2 and 70% N_2O. A dorsal incision was made lateral to the spine and the abdominal cavity was entered. Blood vessels were ligated and spleen was removed by transecting the vessels distal to the ligature. Body temperature was maintained at 37°C throughout surgery using a

feedback-controlled heating pad. Mice were kept under controlled conditions until they were fully recovered from anesthesia.

Soluble mouse RAGE production. Soluble RAGE recombinant baculovirus was a kind gift from Dr. Ann-Marie Schmidt (New York University Langone Medical Center, USA). sRAGE recombinant virus was propagated in Sf21-cells and supernatant was kept at 4°C for further analysis and protein production. Low passage viral titer was determined by quantitative PCR (*42*). For protein production, Sf21 cells were seeded one day prior to infection with 1x106 cells/mL. Cells were infected and incubated at 27°C. Three days later, supernatant (SN) was harvest, filtered and buffer exchanged to 0.1 PBS pH 6.9/50mM NaCl. sRAGE was captured by ion-exchange chromatography using a CaptoS-5mL prepacked column (GE Healthcare) and eluted with 0.1xPBS, pH 6.9/600mM NaCl. Positive fractions were pooled, diluted 15-fold in 0.1PBS pH6.9/50mM NaCl and purified by ion-exchange chromatography using a ResourceS-1mL prepacked column (GE Healthcare). Positive fractions were pooled, dialyzed against PBS, pH 7.2, 10% glycerol at 4°C and stored at -80°C.

Drug & dye administration.

sRAGE: Mice received intraperitoneally three injections of sRAGE (Helmholtz), 30 min before, 24 h and 2 weeks after surgery. sRAGE was injected i.p. at a dose of 3.5 mg kg^{-1} body weight in a final volume of 100 µl.

HMGB1: Mice received one bolus (100µg) of either anti-HMGB1 or isotype control IgG immediately after ischemia induction. The anti-HMGB1 antibody (m2G7, IgG2b) does not recognize HMGB2 and binds to the amino acids 53-63 within the box A domain of rodent and human HMGB1 (*43*) and was purified from hybridoma supernatant by protein G affinity chromatography. The absence of endotoxin contamination was verified by Limulus assay. Recombinant HMGB1 (rHMGB1) in fully-reduced and disulfide redox-state (HMGBiotech) was injected intraperitoneally (one bolus: 5 µg of each redox form (in total 10 µg) in a final volume of 100 µl PBS).

Bromodeoxyuridine (BrdU): BrdU (BD Pharmingen) was administered using osmotic mini-pumps implanted subcutaneously (Alzet model 1002) at a dose of 50µg/d for one week. Osmotic pumps were implanted immediately after stroke or sham surgery.

Qtracker 655: Qtracker 655 (Life technologies) was injected with a 10 µl microsyringe (Hamilton) directly into the femoral bone marrow at the corpus femoris 2 h before stroke or sham surgery at a total volume of 2 µl. Administration of sterile PBS was used as a control.

Adoptive myeloid cell transfer. Donor animals (CCR2 $^{RFP/+}$ or CCR2 $^{RFP/RFP}$) were sacrificed and hind limbs were collected in Dulbecco's Modified Eagle Medium (DMEM). The muscle tissue was removed with 70 % ethanol in a petri dish. The bone marrow was flushed out of femur and tibia with DMEM using a syringe and the cell suspension was filtered through 40 µm cell strainers. After cells were washed and counted they were intraperitoneally injected in *ApoE*$^{-/-}$ recipient mice (10^7 cells per mouse) in a total volume of 200µl in saline.

Molecular MRI imaging with VCAM-1-targeted micron-sized iron oxide particles (MPIOs). MRI Experiments were carried out on a Pharmascan 7 T/12 cm system using surface coils (Bruker, Germany). Before imaging, the mice received an intravenous injection of 1 mg/kg of VCAM-1 targeted MPIOs through a tail vein catheter, as previously described (*22*). Thirty minutes thereafter, 3D T2*-weighted gradient echo imaging with flow compensation (GEFC, spatial resolution of 93µm x 70µm x 70µm interpolated to an isotropic resolution of 70 µm) using respiratory and cardiac gating (images were acquired during the end diastole), with TE/TR 6.2ms/~200ms and a flip angle (FA) of 20° was performed to visualize MPIOs bound to the aortic valve (acquisition time=8-15 min). During MRI, the mice were maintained under anesthesia with 2% isoflurane in 100% O2. For image analysis, the first step was to crop the initial MRI in a 70x70 pixels picture, including the aortic valve and the surrounding blood. Then, 3D Otsu automated threshold was applied using ImageJ software and the signal void volume was computed in mm3.

Organ and tissue processing. Mice were deeply anaesthetized with ketamine (120 mg/kg) and xylazine (16 mg/kg) and venous blood was drawn via cardiac puncture of the right ventricle in 50mM EDTA (Sigma-Aldrich); the plasma was isolated by centrifugation at 3000 relative centrifugal force (rcf) for 10min and stored at -80 °C until further use. The blood pellet was resuspended in DMEM and erythrocytes were lysed using isotonic ammonium chloride buffer. Mice were then transcardially perfused with normal saline and aorta, heart, femurs and spleen were dissected. Spleen and femurs were transferred to Hank's balanced salt solution, homogenized and filtered through 40 µm cell strainers. Erythrocytes in spleens were lysed using isotonic ammonium chloride buffer.

To isolate mononuclear cells from aorta, the whole aorta was minced into small pieces and incubated in Roswell Park Memorial Institute (RPMI) medium containing 125 U/ml collagenase XI, 60 U/ml hyaluronidase I, 60 U/ml DNase I and 450 U/ml collagenase I (Sigma Aldrich) for 30min at 37 °C (*44*). The cell suspensions were then mechanically homogenized, filtered and washed prior to flow cytometry.

Infarct volumetry. Mice were sacrificed by over dose of ketamine-xylazine and perfused intracardially with 10 mL saline solution. Brains were removed and immediately frozen in powdered dry ice. Afterwards, brains were fixed in optimum cutting temperature compound (O.C.T., Tissue-tek) solution and 20µm coronal sections were cut on every 400µm. Sections were stained with cresyl violet and scanned at 600 dpi. Infarct area on each section was analyzed by ImageJ software (NIH). The Swanson method was applied to indirectly measure the infarct area and to correct for cortical swelling: [ischemic area] = [area of the contralateral hemisphere] - [nonischemic area of the ipsilateral hemisphere]. The total infarct volume was determined by integrating measured areas and distances between sections.

Monocyte activation assay. Splenic monocytes were isolated using $CD11b^+$ magnetic-activated cell sorting (CD11b Micro beads, Miltenyi) and cultured (DMEM, 10 % FCS, 1 % Penicilin/Streptavidin) in 12-well flat-bottom plates ($5x10^5$ cells per well). Purity of monocyte

Magnetic-activated cell sorting isolation was verified by flow cytometric analysis to be ≥ 95 %. Treatment with rHMGB1 (0.1 and 0.5 µg/ml), murine stroke or sham plasma (50 % in DMEM) was given in each well individually and 4 h later cells were harvested and prepared for further analysis.

In vitro murine aortic endothelium stimulation assay. Murine aortic endothelial cells (Innoprot, Ref: P10427) were seeded in fibronectin-coated 12-well flat-bottom plates ($5x10^5$ cells per well, Basal medium, 5 % FCS and 1 % Penicillin/Streptavidin, 1 % endothelial cell growth supplement) overnight. Cells were starved for 4 h (basal medium, 1 % Penicillin/Streptavidin) and before they received treatment (recombinant TNF-α: 20 ng/ml, plasma: 50 % in DMEM, recombinant HMGB1: 0.5 µg/ml). The plasma used to stimulate MAECs was collected from stroke- or sham-operated mice 4 h post-lesion. After a 4 h stimulation interval, cells were trypsinized, harvested, washed in PBS and stored at -20°C until further analysis.

Flow cytometry analysis. The following anti-mouse antibodies were used for cell stainings: anti-CD3 (clone: 17A2, eBioscience), anti-CD4 (clone: RM4-5, eBioscience), anti-CD45 (clone: 30-F11, eBioscience), anti-CD11b (clone: M1/70, eBioscience), anti-CD11c (clone: HL3, eBioscience), anti-Ly6C (clone: HK1.4, eBioscience), anti-Ly6G (clone: RB6-8C5, eBioscience), anti-MHC class II (clone: NIMR-4, eBioscience), anti-CCR2 (clone: FAB5538A, R&D systems), BrdU (clone: MOPC-21, BD Biosciences). Stainings were performed according to the manufacturer's protocols. Flow cytometric data was aquired on a BD FACSverse flow cytometer (BD Biosciences) and analyzed using FlowJo software (Treestar).

Oil Red O lipid staining. For whole aorta en face stainings, aortas were carefully dissected and adventitial fat was thoroughly trimmed away. Aortas then were cut open, unfolded, and pinned out on a silicon-elastomer for fixation in 4% paraformaldehyde (PFA) at 4 °C overnight. The aortas then were washed for 4 h in PBS, afterwards placed in 100 % propylene

glycol for 2 min at 25 °C and finally transferred to 0.5 % Oil Red O for 3 h at 25 °C. Then aortas were washed in 85 % propylene glycol and stored in PBS until image acquisition (*45*). For lipid stainings of aortic valve sections, the ventricles were removed horizontally from dissected hearts, embedded in O.C.T compound (Tissue Tek) and consecutively cryosectioned. Sections were dried, post-fixed in 4 % PFA and stained after dehydration for 1 h in 0.5 % Oil Red O solution at 37 °C. Finally, sections were counterstained for nuclei with Mayer's Hematoxylin, air dried and mounted with pre-warmed gelatin (*45*). For lipid staining of the common carotid artery branches, the carotid bifurcation area was dissected and embedded in OCT. compound. After consecutive sectioning, lipid depositions were stained with the same Oil Red O staining protocol as stated above.

Quantification of cap thickness and plaque rupture. Aortic valve sections stained with Oil Red O and Hematoxylin were microphotographed and cap thickness was assessed. Three to five measurements representing the thinnest part of the cap were averaged for each plaque (*46*). Acute plaque rupture was accepted when a visible defect in the cap was accompanied by intrusion of erythrocytes in the plaque. In some animals, 1 or more buried fibrous caps were seen within the body of plaque which were also counted as a plaque rupture (*16*).

MMP 2 and 9 *in situ* zymography of aortic valve sections. DQ-gelatin (D12054, Invitrogen) was dissolved in reaction buffer (50 mM Tris-HCl, 150 mM NaCl, 5 mM CaCl2, 200 mM sodium azide, pH 7.6). Cryosections were incubated for 3 h at 37 °C with the gelatin-containing reaction buffer. Negative control sections were pre-incubated for 1 h with the MMP-inhibitor 1,10-Phenathroline (Sigma). Nuclei were stained with DAPI. MMP activity was detected on an Axio Observer Z1 microscope with 10x magnification and a Fluorescein isothiocyanate (FITC) filter (Carl Zeiss). Data were expressed as MMP+ area(μm^2) and normalized MMP intensity (Normalized MMP intensity = Integrated Density – (Selected valve Area x Background mean fluorescence).

Tyrosine hydroxylase (TH) stainings. Dissected femurs (see above) were decalcified in 0,4 M ethylenediaminetetraacetic acid (EDTA, pH 7.4) for 72 hours. Femurs then were embedded in OCT compound (Tissue Tek) and consecutively sectioned. Sections were blocked with 10 % goat serum and 1 % bovine serum albumin (BSA) for 2 h. After washing with 0,025 % Triton X-100 in TBS, sections were incubated with an antibody against TH (rabbit, abcam) overnight at 4 °C. After washing, sections were then incubated with secondary antibody against rabbit (alexa-647, goat, DAKO) for 90 min at room temperature. Nuclei were stained with DAPI. Pictures were acquired with a confocal microscope at 40x magnification (LSM 880 Carl Zeiss).

Enzyme linked immunosorbent assay. HMGB1 levels were measured from diluted plasma samples (1:10) using a commercial assay kit according to the manufacturer's instructions (IBL international, Hamburg). For CCL-2 levels diluted samples (1:10) were measured using an ELISA kit according to a standard protocol (eBioscience).

Quantitative real time PCR (RT-PCR). Total RNA was purified from aorta, spleen, murine aortic endothelial cells (MAECs) and isolated monocytes using a RNeasy Mini Kit (Qiagen). Equal amount of RNA from each sample was used for cDNA synthesis using High Capacity cDNA Reverse Transcription Kit (Applied Biosystems). The quantitative expression of different cytokines was measured by quantitative real-time PCR with the LightCycler 480 II (Roche) and RT^2 qPCR Primer Assays and SYBR Green ROX qPCR Mastermix (Qiagen).

Primer sequences:

IL-1β: forward ‘5-ACAGATGAAGTGCTCCTTCCA-3’, reverse ‘5-GTCGGAGATTCGTAGCTGGAT-3’

IL-6: forward ‘5-CAGTTGCCTTCTTGGGACTGA-3’, reverse ‘5-GGGAGTGGTATCCTCTGTGAAGTCT-3’

TNF-α: forward 5'-CAT CTT CTC AAA ATT CGA GTG ACA A-3', reverse5'-TGG GAG TAG ACA AGG TAC AAC CC-3'

IFN-γ: forward 5'-TGGCATAGATGTGGAAGAAAAGAG-3', reverse 5'-TGCAGGATTTTCATGTCACCAT-3'

ICAM-1: forward 5′-CAATTTCTCATGCCGCACAG-3′, reverse 5′-AGCTGGAAGATCGAAAGTCCG-3′

VCAM-1: forward 5′-TGAACCCAAACAGAGGCAGAGT-3′, reverse 5′-GGTATCCCATCACTTGAGCAGG-3'

RAGE: forward 5´-GGACCCTTAGCTGGCACTTAGA-3´, reverse5´-GAGTCCCGTCTCAGGGTGTCT-3´

PPIA: forward '5-ACGCCACTGTCGCTTTTC-3', reverse '5-ACCCGACCTCGAAGGAGA-3'

GAPDH: forward 5'-TGACGTGCCGCCTGGAGAAA-3', reverse 5'-AGTGTAGCCCAAGATGCCCTTCAG-3'

RT-PCR array. The RT^2 PreAMP cDNA syntesis Kit (Qiagen) was used for the cDNA synthesis and RT^2 Profiler PCR Array for chemokines and chemokine receptors (PAMM-022Z, Qiagen) was measured in a Roche LightCycler 480. Finally, data was analyzed with RT^2 Profiler PCR Array Data analysis software (version3.5) from SABiosciences.

Quantification of patient infarct volumes. Infarct volumes were quantified on images from diagnostic scans, either computed tomography or magnetic resonance imaging (diffusion-weighted, T2 or fluid-attenuated inversion recovery). The modality and image with the largest infarct size was used for volumetry. Trained raters segmented infarcts manually slice-by-slice. The inter-rater reliability for this procedure showed an intraclass correlation coefficient of 0.993.

Analysis of HMGB1 isoforms by electrospray ionization liquid chromatography tandem mass spectrometry (ESI-LC-MS/MS). Samples were pre-cleared with 50 µl protein G-Sepharose beads for 1h at 4°C and HMGB1 present was immunoprecipitated with 5 µg of rabbit anti-HMGB1 (ab18256) for 16 h at 4°C as previously described (*47*). For the analysis

of HMGB1 post translational modifications, free thiol groups within HMGB1 were alkylated for 90 min with 10 mM iodoacetamide at 4°C. Cysteine residues in disulfide bonds were then reduced with 30 mM dithiothreitol at 4°C for 1 h followed by alkylation of newly exposed thiol groups with 90 mM NEM at 4°C for 10 min as previously described (*33, 48*). Samples were subjected to trypsin (Promega) or GluC (New England Biolabs) digestion according to manufacturer's instructions and de-salted using C18 zip-tips (Millipore). Characterization of post translational modifications within HMGB1 were determined as described previously using an AB Sciex QTRAP 5500 (Sciex Inc.) equipped with a NanoSpray II source by in-line liquid chromatography using a U3000 HPLC System (Dionex), connected to a 180 µm x 20 mm nanoAcquity UPLC C18 trap column and a 75 µm x 15 cm nanoAcquity UPLC BEH130 C18 column (Waters) via reducing unions. A gradient from 0.05% TFA (v/v) to 50% ACN/0.08% TFA (v/v) in 40 min was applied at a flow rate of 200 nL/min (*49*). The ion spray potential was set to 2,200-3,500 V, the nebulizer gas to 19 L/min and the interface heater to 150°C. Accurate mass and whole protein electrospray ionisation (ESI) mass spectrometry is determine as previously described using a AB Sciex TripleToF 5600+ system (*49*).

Supplementary Figures

Figure S1

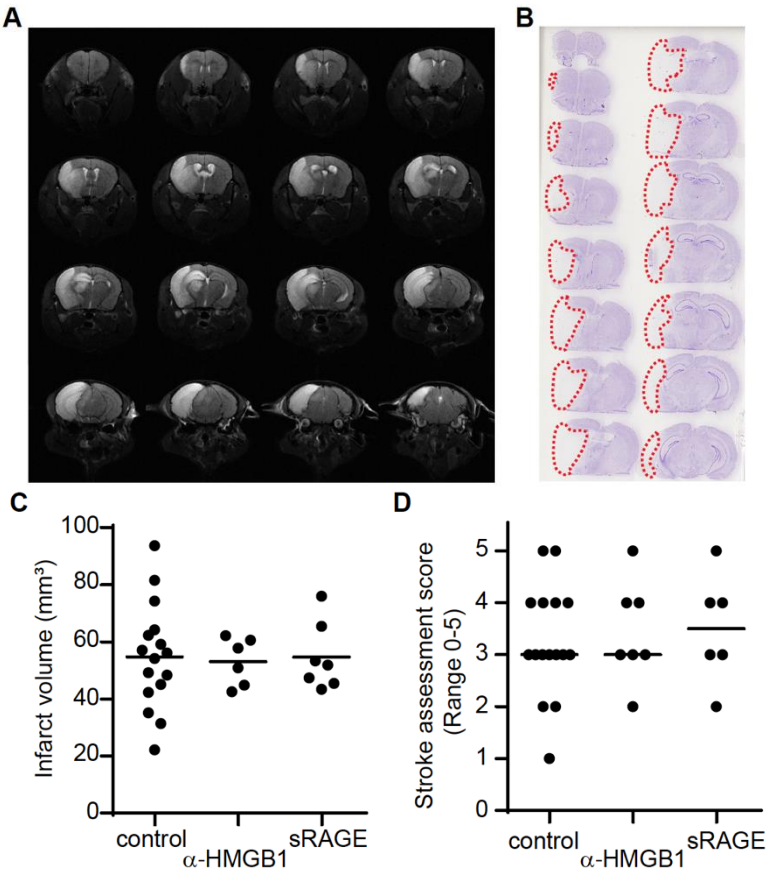

Figure S1. Characterization of the 60-min filament MCA occlusion (fMCAo) model. (**A**) Coronal brain sections from T2w MRI of an in infarcted brain 5 days after 60 min fMCAo surgery. (**B**) Cresyl violet histology of coronal sections of an infarcted brain 7 days after fMCAo. (**C**) Quantification of brain infarct volume cresyl violet histology of a untreated compared to anti-HMGB1 antibody and sRAGE treated brains. (**D**) Comparison of stroke assessment scores 1 h after reperfusion in fMCAo mice (n= 6-16 per group). All mice used are HCD-fed ApoE$^{-/-}$ mice.

Figure S2

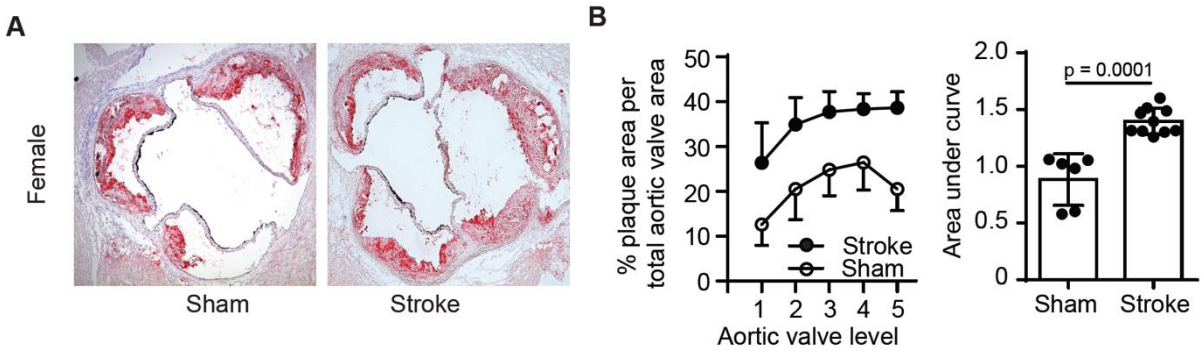

Figure S2. Exacerbation of atherosclerotic lesions in aortic valves of male and female HCD-fed *ApoE*$^{-/-}$ mice 1 month after fMCAo surgery. (**A**) Representative images of Oil Red O aortic valve quantification of female HCD-fed ApoE$^{-/-}$ mice one month after stroke or sham surgery. (**B**) Plaque area quantification of 5 consecutive levels in aortic valves (left) and area under curve (AUC, right) analysis in stroke and sham-operated mice one month after surgery (U Test, 8-10 per group). All data in panel B are shown as mean with error bars indicating s.d.

Figure S3

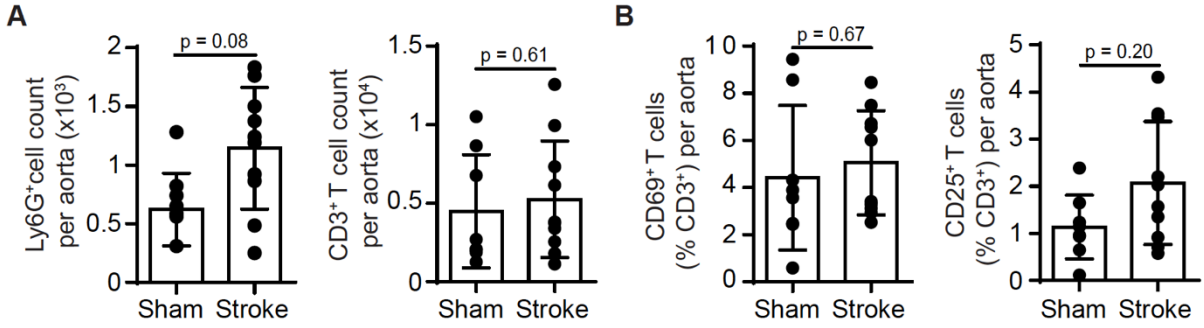

Figure S3. Immune cell counts in aorta of HCD-fed *ApoE*$^{-/-}$ mice 1 month after experimental stroke. (**A**) CD45^{+}Ly6G^{+} granulocytes (left) and CD45^{+}CD3^{+} T cells (right) cell counts after sham or stroke surgery. (**B**) Percentage of CD69^{+} (left) and CD25^{+} (right) T cell subsets after sham or stroke surgery. (U Test, n= 8-10 per group).

Figure S4

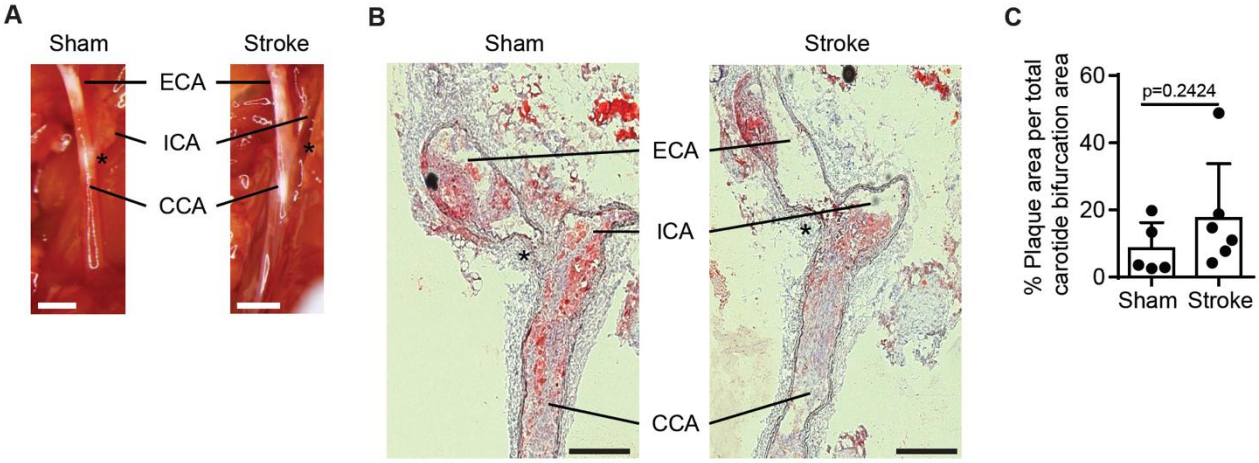

Figure S4. Analysis of atherosclerotic plaque load at the common carotid artery bifurcation in HCD-fed *ApoE*$^{-/-}$ mice. (**A**) Representative microphotographs of the common carotid artery bifurcation on the contralateral side 7 days after stroke or sham surgery (scale bar = 1mm, * indicates bifurcation). (**B**) Representative Oil Red O stained longitudinal common carotid artery bifurcation sections (scale bar = 500µm, * indicates bifurcation). (**C**) Quantification of Oil Red O+ plaque load in the contralateral common carotid artery lumen 7 days after stroke or sham surgery (U Test, n= 5-6 per group). CCA = common carotid artery, ICA = internal carotid artery, ECA = external carotid artery.

Figure S5

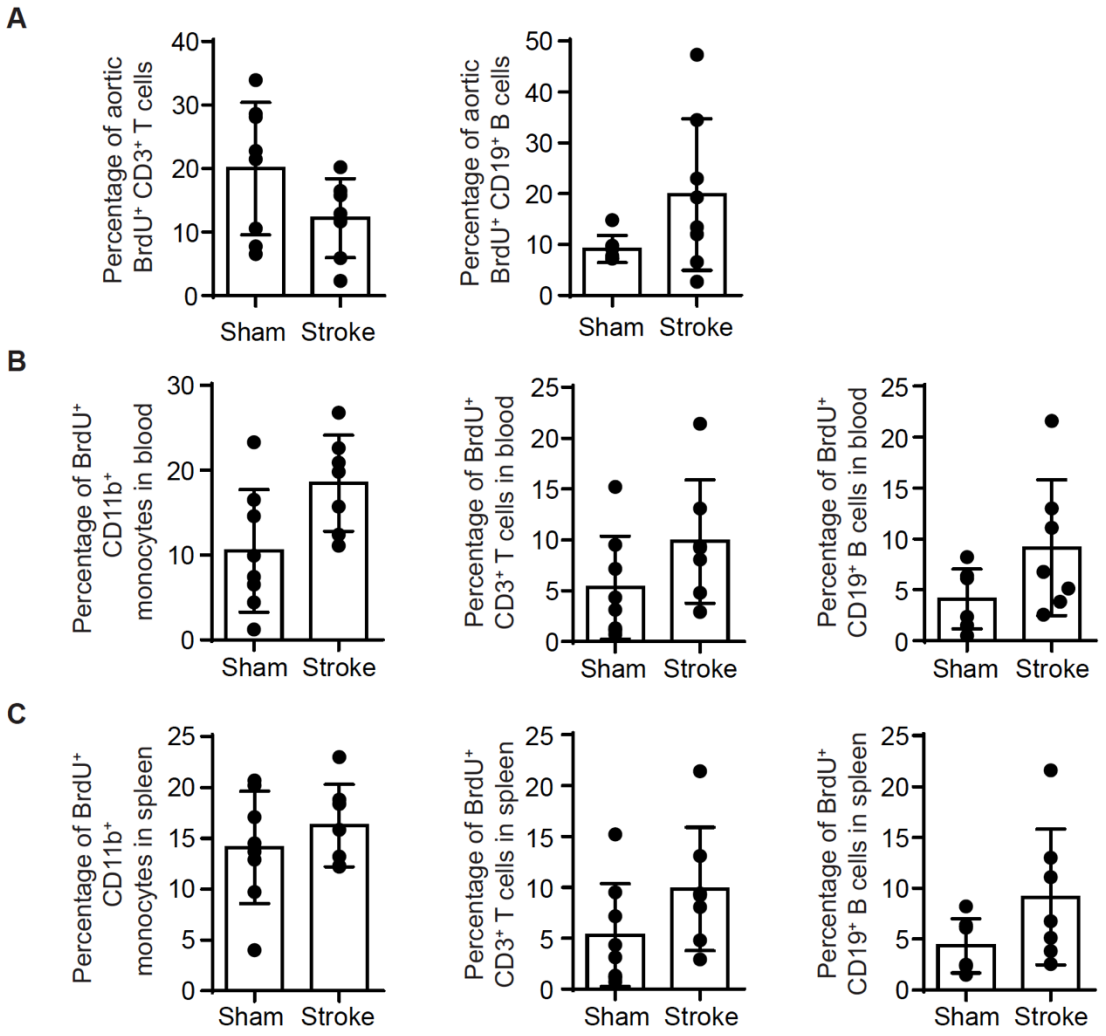

Figure S5. Comparison of BrdU incorporation in aorta, blood, and spleen 1 week after experimental stroke surgery. (A) Percentage of $BrdU^+$ $CD3^+$ T cells (left) and $BrdU^+$ $CD19^+$ B cells in aorta after stroke or sham surgery. (B, C) Percentage of $BrdU^+$ cells in blood (**B**) and spleen (**C**) after experimental stroke or sham surgery (U Test, n= 6-8 mice per group). All bar graphs are shown as mean ± s.d.

Figure S6

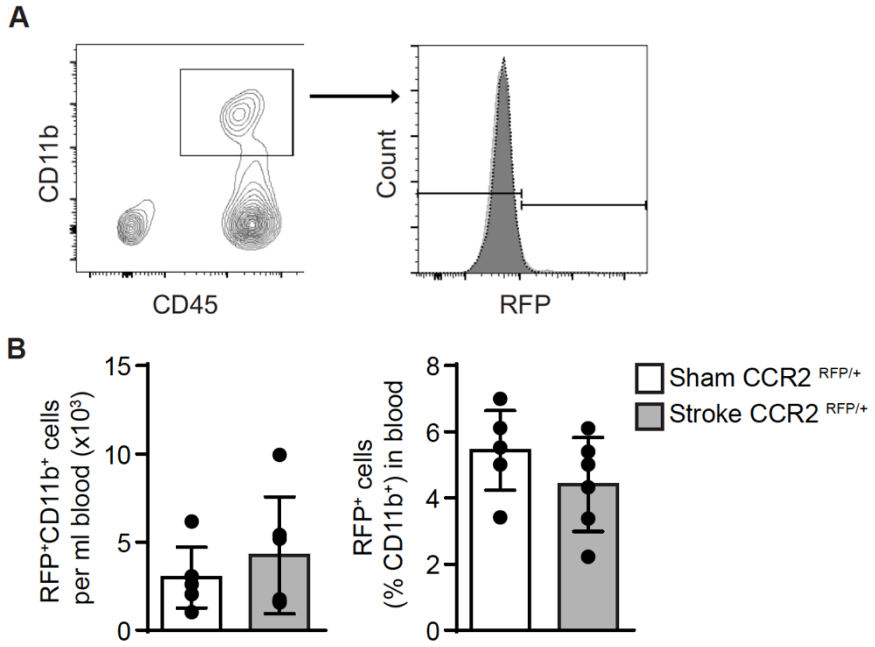

Figure S6. RFP$^+$CD11b$^+$ cell counts in blood after experimental stroke surgery. HCD-fed ApoE$^{-/-}$ mice underwent sham or stroke surgery received CCR2RFP/+ bone marrow cell (BMC) transplantation (10^7 cells) immediately after surgery. One week later mice were sacrificed and blood analyzed. (**A**) Flow cytometric gating strategy to analyze RFP$^+$CD11b$^+$ cells in blood. (**B**) Quantification of total RFP$^+$CD11b$^+$ cell counts in blood one week after sham or stroke surgery (left). Percentage of RFP$^+$CD11b$^+$ cells in blood one week after sham or stroke surgery (right, U Test, n= 5-6 mice per group). All bar graphs are shown as mean ± s.d.

Figure S7

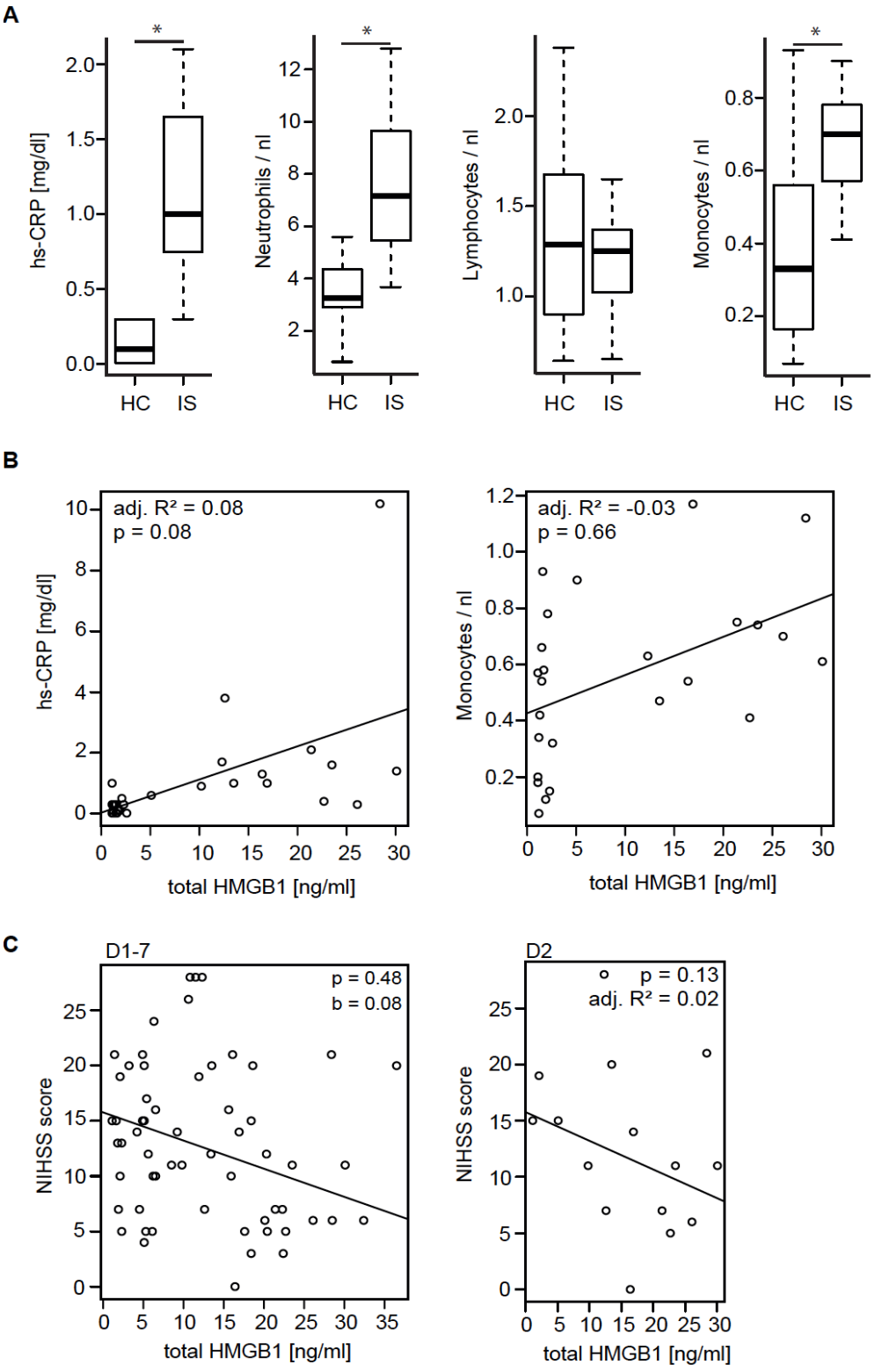

Figure S7. Immunological data of stroke patients. (**A**) Comparison of hs-CRP and leukocyte subpopulations between HCs and patients with IS at day 2 (Wilcoxon rank sum test) (**B**) Regression of total HMGB1 levels with hs-CRP or monocytes/nl of HCs and IS patients at day 2 after stroke (Linear regression analysis with adjustment for groups). (**C**) Regression analysis of NIHSS scores and total HMGB1 levels in patients with IS from admission to day 7 after stroke (Linear mixed model with day as random effect). Abbreviations: NIHSS, National Institute of Health stroke scale; IS, ischemic stroke.

Figure S8

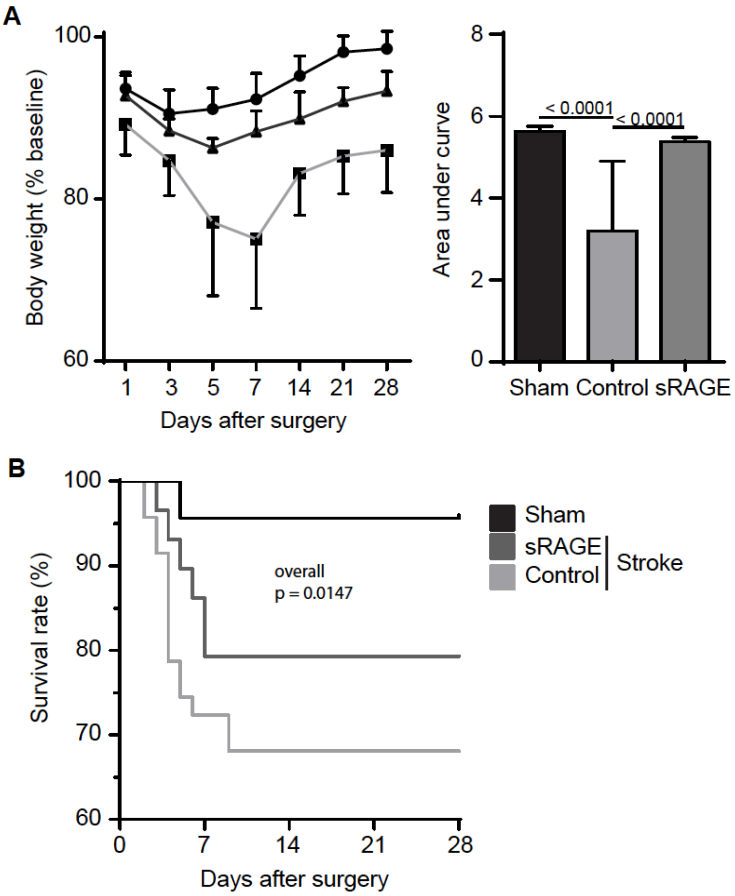

Figure S8. Body weight and mortality in sRAGE treatment mice after stroke. (**A**) Body weight curves (left, indicated as % body weight to individual baseline before stroke) after sham and stroke surgery with vehicle or sRAGE treatment. Area under curve analysis (right) for statistical analysis of indicated groups (U Test, n= 10-15 mice per group, graphs shown as mean ± s.d.). (**B**) Kaplan-Meier curves of post-stroke survival within one month after stroke in vehicle or sRAGE treated and sham-operated mice (Comparison of differences between curves by Mantel-Cox Test , n= 28-47).

Figure S9

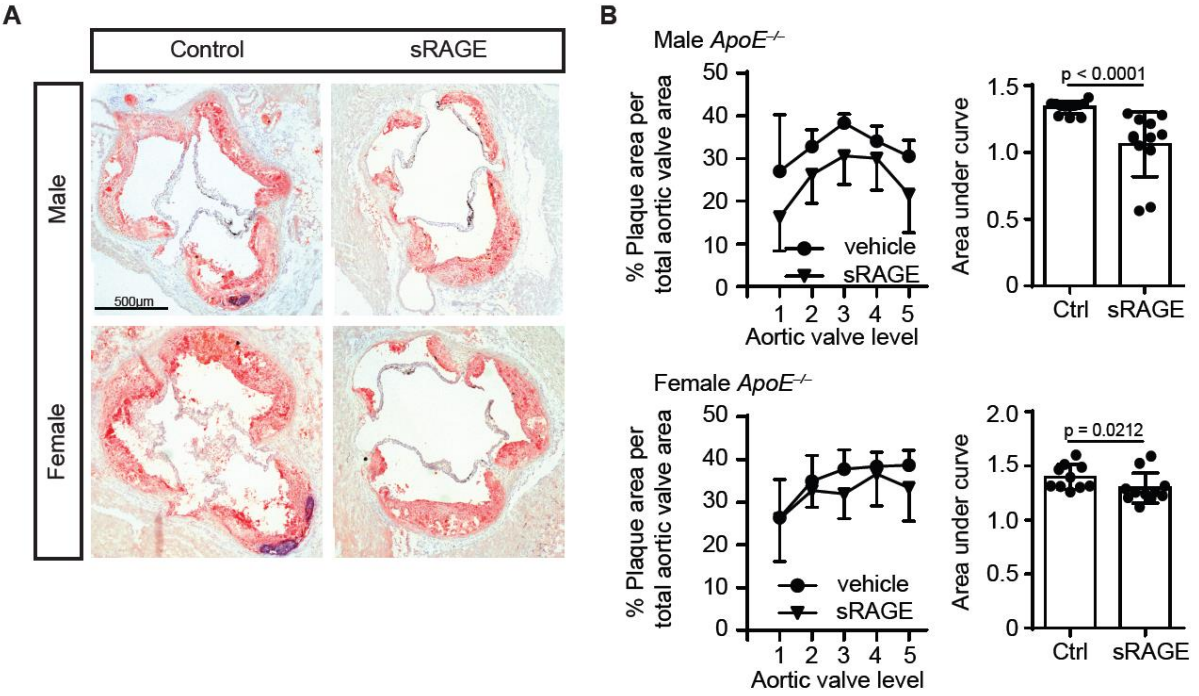

Figure S9. Atherosclerotic lesions in aortic valves of male and female HCD-fed ApoE$^{-/-}$ mice 1 month after experimental stroke and sRAGE treatment. (**A**) Representative images of Oil Red O aortic valve sections of male and female HCD-fed ApoE$^{-/-}$ mice with vehicle or sRAGE treatment 4 weeks after stroke surgery. (**B**) Plaque area quantification of 5 consecutive levels in aortic valves and area under curve (AUC) analysis of stroke (± sRAGE) for male and female mice (U Test, n= 8-10 mice per group). All graphs are shown as mean with error bars indicating s.d.

Figure S10

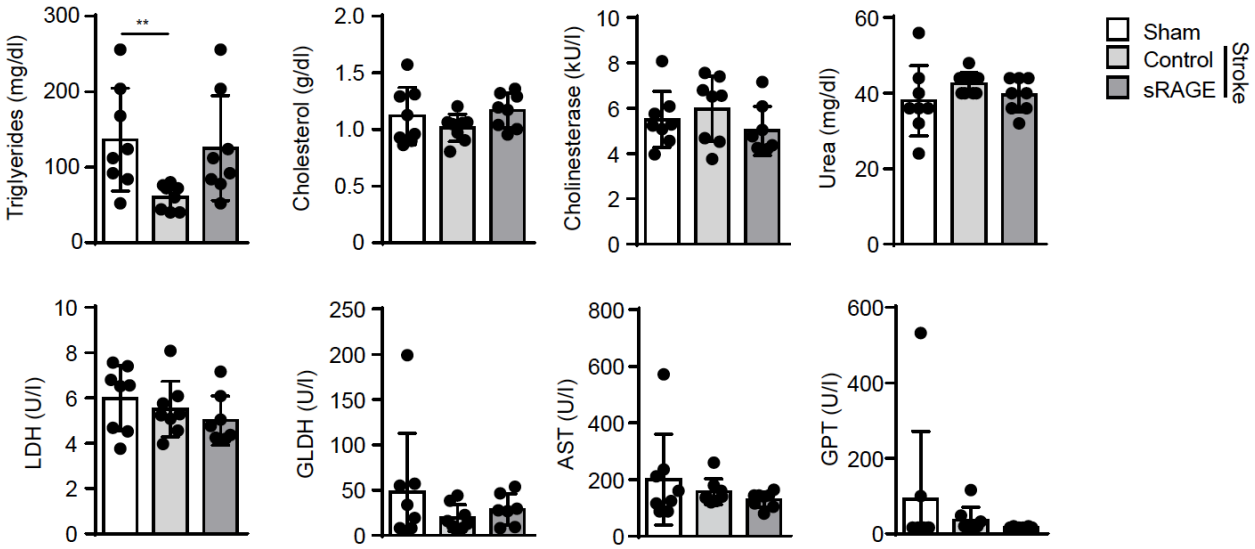

Figure S10. Lipid profile of plasma samples 1 month after experimental stroke surgery and sRAGE treatment. Triglycerides, cholesterol, cholinesterase, urea, lactate dehydrogenase (LDH), glutamate dehydrogenase (GLDH), aspartate aminotransferase (AST) and glutamic pyruvic transaminase (GPT) concentrations after experimental stroke or sham surgery (± sRAGE) in HCD-fed ApoE$^{-/-}$ mice. (One way-ANOVA; n= 8-9 mice per group). All bar graphs are shown as mean ± s.d.

Figure S11

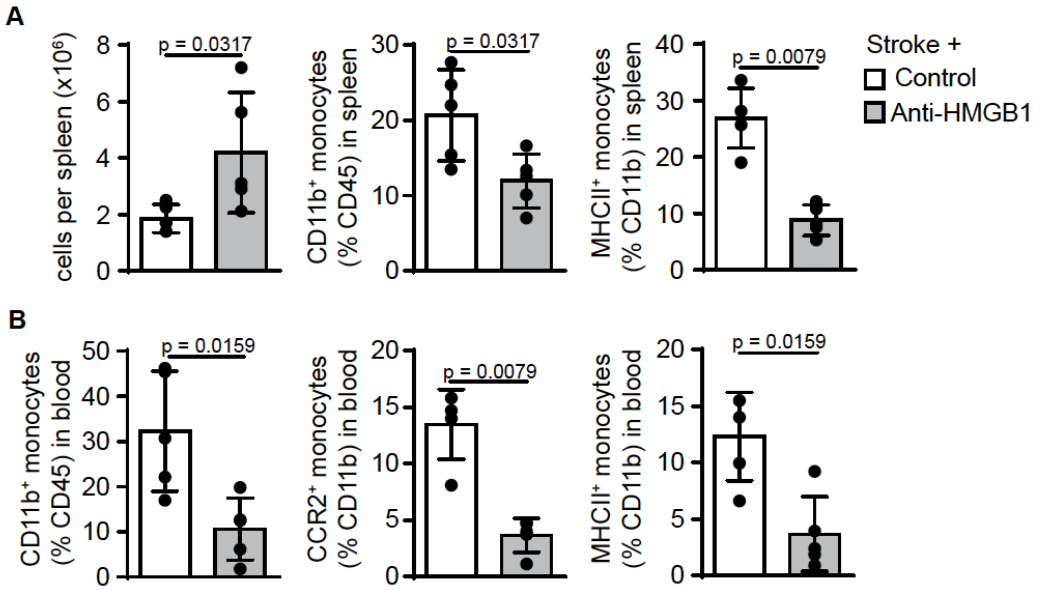

Figure S11. Flow cytometric analysis of spleen and blood 24 hours after experimental stroke with anti-HMGB1 treatment. (**A**) Flow cytometric analysis of WT mice treated with IgG control or HMGB1-specific monoclonal antibodies (anti-HMGB1) 24 h after stroke surgery. Whole $CD45^+$ spleen cell counts (left) and percentages of $CD11b^+$ (middle) and $CD11b^+MHCII^+$ (right) cells were measured. (**B**) Flow cytometric analysis of $CD45^+CD11b^+$ (left), $CD11b^+CCR2^+$ (middle) and CD11b+MHCII+ (right) cell percentages from blood 24 h after stroke ± anti-HMGB1 treatment (U Test, n= 5-8 mice per group). All bar graphs are shown as mean ± s.d.

Figure S12

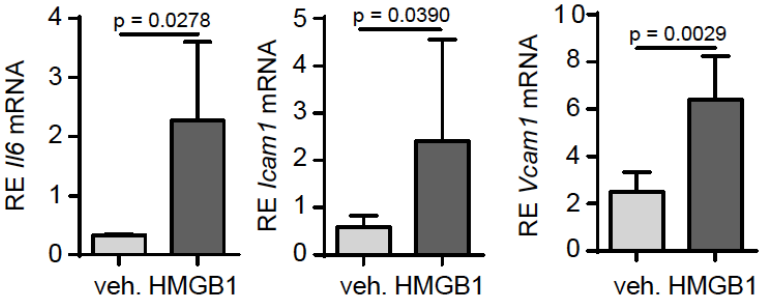

Figure S12. Recombinant HMGB1 in vivo administration exacerbates atherosclerosis. HCD-fed ApoE$^{-/-}$ mice received i.p. injection of a single bolus of 10 µg rHMGB1. After one week mice were sacrificed and aorta and aortic valve were analyzed. Expression of *Il-6* (left), *Icam-1* (middle) and *Vcam-1* (right) (RE, relative expression) was analyzed from aorta lysates (U Test, n= 5 per group). All graphs are shown as mean ± s.d.

Figure S13

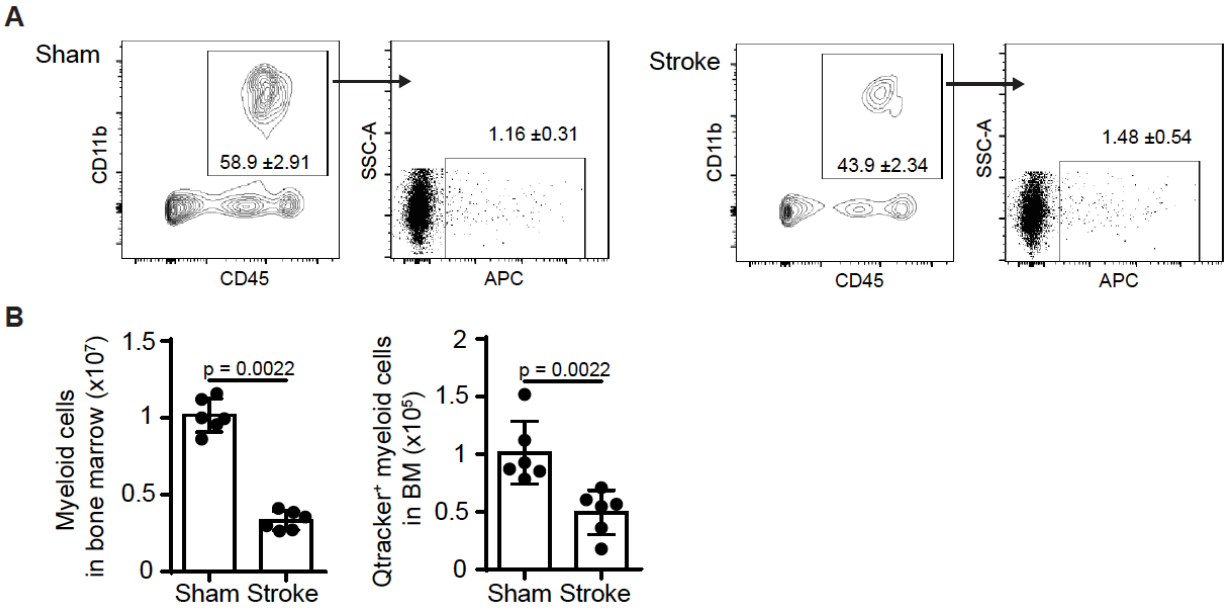

Figure S13. Quantification of in vivo Qdot labeling of femoral bone marrow 24 hours after experimental stroke. WT mice received Qdot administration in the femoral bone marrow 2h before sham or stroke surgery and were sacrificed 24 h later. (**A**) Representative gating strategy for $CD45^{+}CD11b^{+}$ monocytes and Qdot+ monocytes in femoral bone marrow after stroke or sham surgery. (**B**) Quantification of myeloid cells (left) and Qdot+ monocytes (right) in femoral bone marrow (U Test, n= 6 per group). All graphs are shown as mean ± s.d.

Figure S14

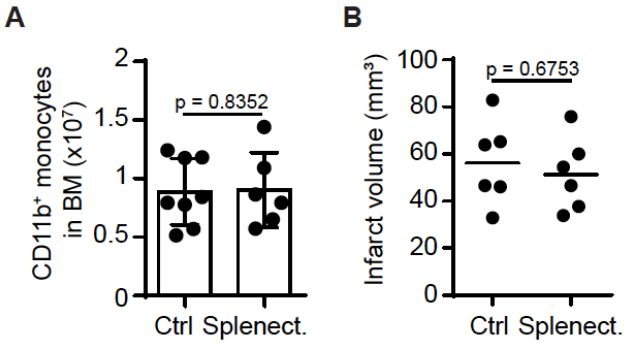

Figure S14. Myeloid cell count in femoral bone marrow and brain infarct volumetry after splenectomy. Spleen of HCD-fed ApoE$^{-/-}$ mice were removed surgically or sham surgery was performed before experimental stroke was induced. One week later mice were sacrificed and analyzed for myeloid cell counts and infarct volumetry. (**A**) Flow cytometric analysis of bone marrow from either splenectomized or sham operated mice after experimental stroke (U Test, n= 6-8 per group). (**B**) Cresyl violet histology of infarcted brains from stroked mice with either splenectomy or sham surgery (U Test, n=6 per group). All graphs shown as mean ± s.d.

Figure S15

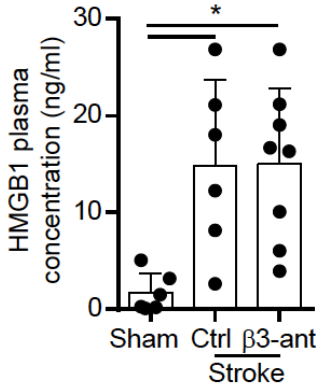

Figure S15. Impact of β3-adrenoreceptor blockage on HMGB1 plasma levels after experimental stroke. HMGB1 plasma concentrations were measured by ELISA in sham and stroke-operated (± SR59230A treatment) HCD-fed ApoE$^{-/-}$ mice 7d after surgery (H Test, n= 6-8 per group). Graph is shown as mean ± s.d. (* = p value <0.05).

Figure S16

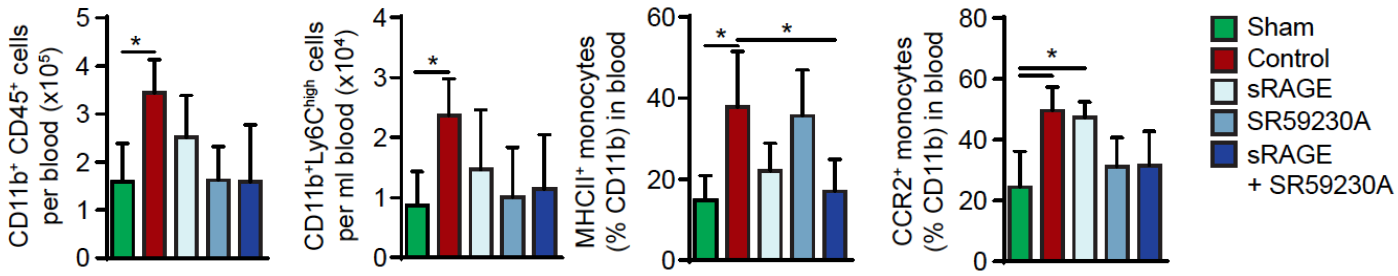

Figure S16. Impact of β3-adrenoreceptor blockage (SR59230A), alarmin blockage (sRAGE), and combined treatment on blood immune cells in WT mice. WT mice received either SR59230A, sRAGE, both combined or control treatment immediately after stroke and blood was analyzed by flow cytometry 24 h later for total myeloid ($CD45^+CD11b^+$), $CD11b^+Ly6C^{high}$, MHCII and CCR2 expressing cells (H Test, n= 6-8 per group). All graphs are shown as mean ± s.d. (*: $p < 0.05$)

Figure S17

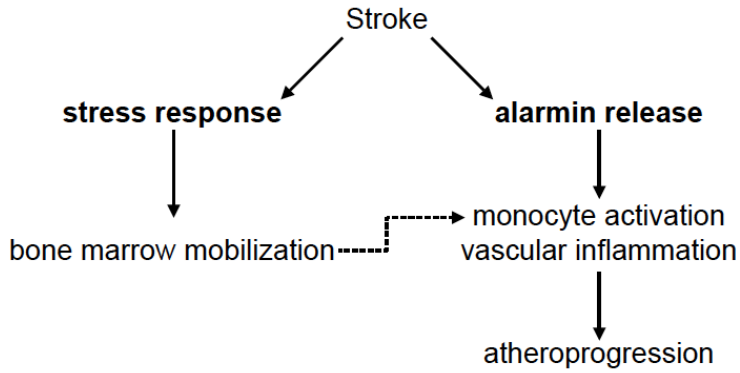

Figure S17. Schematic overview of proposed mechanism of atheroprogression after stroke.

Table S1. Primer list for quantitative PCR array (mouse chemokines and receptors).

Symbol	Description
C5ar1	Complement component 5a receptor 1
Ackr2	Chemokine binding protein 2
Ccl1	Chemokine (C-C motif) ligand 1
Ccl11	Chemokine (C-C motif) ligand 11
Ccl12	Chemokine (C-C motif) ligand 12
Ccl17	Chemokine (C-C motif) ligand 17
Ccl19	Chemokine (C-C motif) ligand 19
Ccl2	Chemokine (C-C motif) ligand 2
Ccl20	Chemokine (C-C motif) ligand 20
Ccl22	Chemokine (C-C motif) ligand 22
Ccl24	Chemokine (C-C motif) ligand 24
Ccl25	Chemokine (C-C motif) ligand 25
Ccl26	Chemokine (C-C motif) ligand 26
Ccl28	Chemokine (C-C motif) ligand 28
Ccl3	Chemokine (C-C motif) ligand 3
Ccl4	Chemokine (C-C motif) ligand 4
Ccl5	Chemokine (C-C motif) ligand 5
Ccl6	Chemokine (C-C motif) ligand 6
Ccl7	Chemokine (C-C motif) ligand 7
Ccl8	Chemokine (C-C motif) ligand 8
Ccl9	Chemokine (C-C motif) ligand 9
Ccr1	Chemokine (C-C motif) receptor 1
Ccr10	Chemokine (C-C motif) receptor 10
Ccr1l1	Chemokine (C-C motif) receptor 1-like 1
Ccr2	Chemokine (C-C motif) receptor 2
Ccr3	Chemokine (C-C motif) receptor 3
Ccr4	Chemokine (C-C motif) receptor 4
Ccr5	Chemokine (C-C motif) receptor 5
Ccr6	Chemokine (C-C motif) receptor 6
Ccr7	Chemokine (C-C motif) receptor 7
Ccr8	Chemokine (C-C motif) receptor 8
Ccr9	Chemokine (C-C motif) receptor 9
Ackr4	Chemokine (C-C motif) receptor-like 1
Ccrl2	Chemokine (C-C motif) receptor-like 2
Cmklr1	Chemokine-like receptor 1
Cmtm2a	CKLF-like MARVEL transmembrane domain containing 2A
Cmtm3	CKLF-like MARVEL transmembrane domain containing 3
Cmtm4	CKLF-like MARVEL transmembrane domain containing 4
Cmtm5	CKLF-like MARVEL transmembrane domain containing 5
Cmtm6	CKLF-like MARVEL transmembrane domain containing 6
Cx3cl1	Chemokine (C-X3-C motif) ligand 1
Cx3cr1	Chemokine (C-X3-C) receptor 1
Cxcl1	Chemokine (C-X-C motif) ligand 1
Cxcl10	Chemokine (C-X-C motif) ligand 10
Cxcl11	Chemokine (C-X-C motif) ligand 11
Cxcl12	Chemokine (C-X-C motif) ligand 12
Cxcl13	Chemokine (C-X-C motif) ligand 13
Cxcl14	Chemokine (C-X-C motif) ligand 14
Cxcl15	Chemokine (C-X-C motif) ligand 15
Cxcl16	Chemokine (C-X-C motif) ligand 16
Cxcl2	Chemokine (C-X-C motif) ligand 2
Cxcl3	Chemokine (C-X-C motif) ligand 3
Cxcl5	Chemokine (C-X-C motif) ligand 5
Cxcl9	Chemokine (C-X-C motif) ligand 9
Cxcr1	Chemokine (C-X-C motif) receptor 1
Cxcr2	Chemokine (C-X-C motif) receptor 2
Cxcr3	Chemokine (C-X-C motif) receptor 3

Cxcr4	Chemokine (C-X-C motif) receptor 4
Cxcr5	Chemokine (C-X-C motif) receptor 5
Cxcr6	Chemokine (C-X-C motif) receptor 6
Ackr3	Chemokine (C-X-C motif) receptor 7
Ackr1	Duffy blood group, chemokine receptor
Fpr1	Formyl peptide receptor 1
Gpr17	G protein-coupled receptor 17
Hif1a	Hypoxia inducible factor 1, alpha subunit
Ifng	Interferon gamma
Il16	Interleukin 16
Il1b	Interleukin 1 beta
Il4	Interleukin 4
Il6	Interleukin 6
Itgam	Integrin alpha M
Itgb2	Integrin beta 2
Mapk1	Mitogen-activated protein kinase 1
Mapk14	Mitogen-activated protein kinase 14
Pf4	Platelet factor 4
Ppbp	Pro-platelet basic protein
Slit2	Slit homolog 2 (Drosophila)
Tgfb1	Transforming growth factor, beta 1
Tlr2	Toll-like receptor 2
Tlr4	Toll-like receptor 4
Tnf	Tumor necrosis factor
Tymp	Thymidine phosphorylase
Xcl1	Chemokine (C motif) ligand 1
Xcr1	Chemokine (C motif) receptor 1
Actb	Actin, beta
B2m	Beta-2 microglobulin
Gapdh	Glyceraldehyde-3-phosphate dehydrogenase
Gusb	Glucuronidase, beta
Hsp90ab1	Heat shock protein 90 alpha (cytosolic), class B member 1

Table S2. Demographic and clinical characteristics of the study population.

Characteristics	Stroke	Control
Demographic characteristics		
Total, n	18	12
Age, mean (SD) [years]	72.7 (14.3)	72.1 (5.9)
Female, n (%)	7 (38.9)	8 (66.7)
Vascular risk factors, n (%)		
Hypertension	15 (83.3)	4 (33.3)
Smoking history	8 (47.1)	3 (25)
Hypercholesterolemia	2 (11.8)	1 (8.3)
Obesity	4 (26.7)	1 (8.3)
Diabetes mellitus	1 (5.6)	0 (0)
Previous TIA/stroke/MI	5 (27.8)	0 (0)
ΔT, mean (SD) [hours]	5.5 (5.6)	n/a
Infarct volumes, mean (SD) [ml]	74.4 (48.0)	n/a

SD, standard deviation; TIA, transient ischemic attack; MI, myocardial infarction; ΔT, time from symptom onset until hospital arrival; n/a, not available.

Table S3. Number of (excluded/included) animals in accomplished experiments.

Experiment	Total animals	Included animals	Excluded animals	Reason for exclusion
Aorta *en face* Oil Red O	20	16	4	Died after surgery
4 w Aortic valve Oil Red O & Aorta Flow cytometry	30	24	6	Died after surgery
BrdU assay	15	14	1	Died during surgery
3 d aorta lysates and CCR2 FACS	14	14	0	-
RFP^{+} transplantation	15	11	2 2	Died after surgery Transplantation failed
RFP^{het} vs. RFP^{hom}	12	11	1	Died after surgery
VCAM1 MRI	10	5	4 1	MRI scan quality Died after surgery
MAEC stimulation	35	35	-	-
HMGB1 1d ELISA	14	14	-	-
3 d sRAGE treatment	24	24	-	-
Monocyte stimulation	25	24	1	Died during surgery
4 w sRAGE treatment	12	8	4	Died after surgery
siRNA assay	28	21	4 3	Failed siRNA injection Died during procedure
Anti-HMGB1 ApoE	24	20	3 1	Died after surgery No infarct detected
Anti-HMGB1 Bl6	20	20	.	-
HMGB1 administration	15	-	-	-
Qdot tracker	14	12	2	Qdot administration failed
Splenectomy	15	14	1	Died during surgery
Beta3-blocker	40	35	3 2	Died during surgery No infarct detected

4 w, 4 weeks; 3 d, 3 days; het, heterozygous; hom, homozygous.